

Study on Control Scheme for the Inverters in Low Voltage Microgrid with Nonlinear Loads

Jiqiang XU¹, Wenzhou LU^{1,a} and Lei WU¹

¹Key Laboratory of Advanced Process Control for Light Industry, Ministry of Education, Jiangnan University, Wuxi, China 214122

^aCorresponding author: luwenzhou@126.com

Abstract. There are a lot of nonlinear loads in real low voltage microgrid system. It will cause serious output voltage and grid current harmonic distortions problems in island and grid-connected modes, respectively. To solve this problem, this paper proposes a droop control scheme with quasi-proportion and resonant (quasi-PR) controller based on $\alpha\beta$ stationary reference frame to make microgrid smoothly switch between grid-connected and island modes without changing control method. Moreover, in island mode, not only stable output voltage and frequency, but also reduced output voltage harmonics with added nonlinear loads can be achieved; In grid-connected mode, not only constant power, but also reduced grid current harmonics can be achieved. Simulation results verify the effectiveness of the proposed control scheme.

1. Introduction

For microgrid, there are four modes, i.e. island, grid-connected and switchings between them [1-2]. In real low voltage microgrid system, there are a lot of nonlinear loads [3]. Thus, microgrid should have the ability of stable operation with nonlinear loads in all these four modes. It is an important problem for its control scheme development [4].

Reference [5] proposed a controller, suitable for grid-connected mode with nonlinear loads, but not for island mode. Reference [6] proposed a control method together with PI and quasi-PR controllers for inverter with nonlinear loads, which is only suitable for island mode. References [7-8] proposed a droop control scheme based on virtual impedance for parallel inverters with nonlinear loads, which is only suitable for single-phase inverter in island mode. Reference [9] proposed a droop control for multiple harmonics with nonlinear loads, which can reduce grid current harmonics in grid-connected mode, but is not good for the reducing of output voltage harmonic in island mode. Reference [10] proposed a droop control method with quasi-PR controller based on abc coordinate system for the parallel inverters with nonlinear loads, but only suitable in island mode. Reference [11] proposed a droop control method with PR controller based on $\alpha\beta$ stationary coordinate system for high-voltage system with nonlinear loads in both island and grid-connected modes, in which the output voltage harmonic distortion is small, but system performance in grid-connected mode is not analyzed.

Based on the references mentioned above, an integrated and improved droop control strategy with quasi-PR controller based on $\alpha\beta$ stationary coordinate system in low-voltage system with nonlinear loads is proposed in this paper. Moreover, virtual impedance for the voltage and current double closed-loop is added to achieve the resistive output impedance of the inverters. Finally, the improved



performance of microgrid with nonlinear loads in four operation modes will be verified through simulation.

2. Droop control with quasi-PR controller of Inverters

2.1. Quasi-PR controller

The proposed control scheme for three-phase inverter in island and grid-connected modes is based on droop control framework, and includes the double control, the virtual impedance implementation, and the quasi-PR controller based on $\alpha\beta$ stationary reference frame. Three-phase reference voltage is given by the droop control equation.

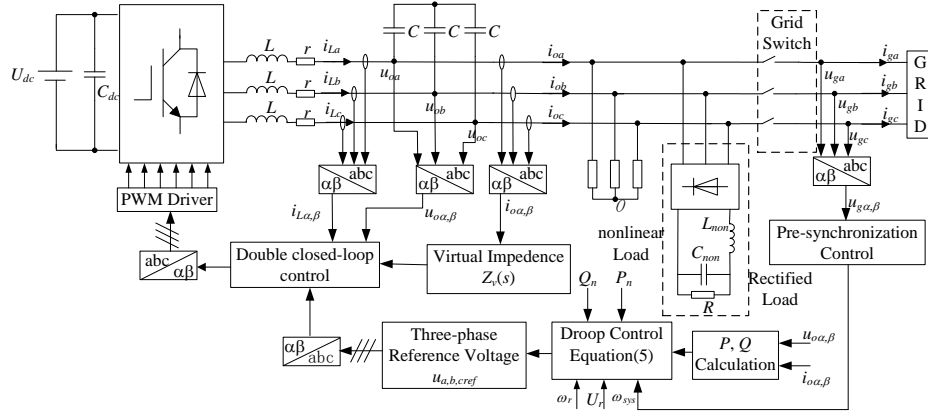


Figure 1. Block diagram of droop control of three inverter with island and grid-connected mode

A three-phase inverter can be simplified into two independent single-phase systems [8]. The simplified diagram of double closed-loop control of inverter is shown in figure 2, which includes a voltage and a current control loop.

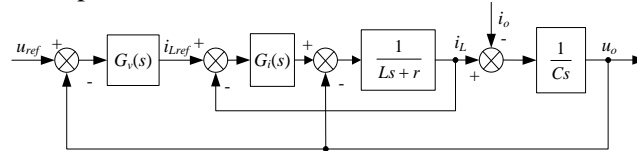


Figure 2. Double closed-loop control of inverter

In figure 2, the outer voltage loop controller $G_v(s)$ adopts quasi-PR controller to achieve static error tracking of output fundamental voltage and suppression of 5th, 7th, 11th and 13th harmonic voltages [10]. The inner current loop controller $G_i(s)$ adopts proportional (P) control of the inductor currents. Thus, the inverter output voltage can be obtained as follows:

$$u_o = G(s)u_{ref} - Z_o(s)i_o = \frac{G_i(s)G_v(s) \cdot u_{ref}}{LCs^2 + C(r + G_i(s))s + G_i(s)G_v(s)} - \frac{(Ls + r + G_i(s)) \cdot i_o}{LCs^2 + C(r + G_i(s))s + G_i(s)G_v(s)} \quad (1)$$

where $Z_o(s)$ is the equivalent output impedance; $G(s)$ is the output voltage transfer function; u_{ref} is the inverter reference voltage; i_o is the inverter output current; L and C are the inverter filter inductance and capacitance; r is the internal resistance of the filter inductor. $G_v(s)$, $G_i(s)$ can be described as follows [11]:

$$G_v(s) = k_{pv} + \sum_{i=1,5,7,11,13} \frac{k_{ri}s}{s^2 + 2\omega_{ri}s + \omega_i^2} \quad (2)$$

$$G_i(s) = k_{pi} \quad (3)$$

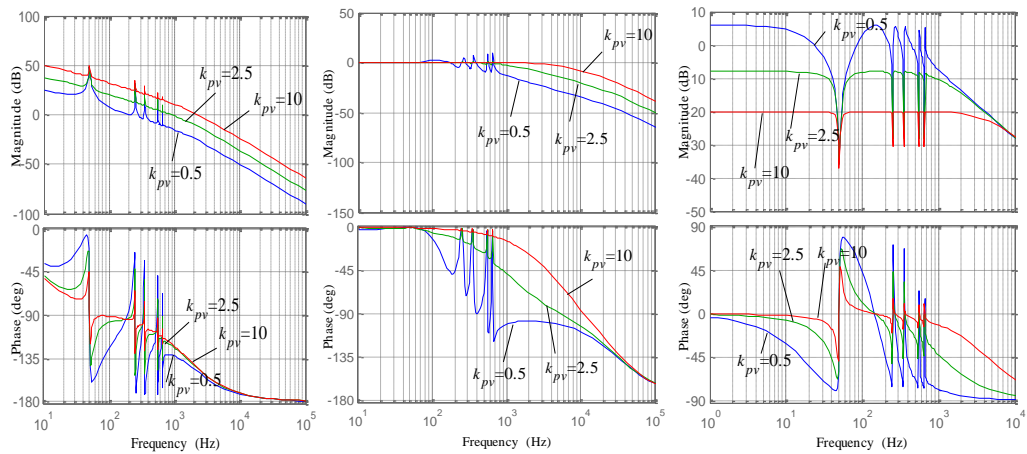
where k_{pv} is the proportional coefficient of quasi-PR controller; k_{ri} and ω_{ri} are the resonance and

bandwidth coefficients for the i^{th} -order ($i=1,5,7,11,13$) harmonic frequency, respectively; k_{pi} is the proportional coefficient of current controller; Fundamental angular frequency $\omega_1=2\pi*50\text{rad/s}$.

In order to analyze the properties of $G_v(s)$, $Z_o(s)$ and $G(s)$, corresponding values are determined as follows: $L=5\text{mH}$, $r=0.02\Omega$, $C=400\mu\text{F}$, $k_{r1}=200$, $k_{r5}=150$, $k_{r7}=100$, $k_{r11}=50$, $k_{r13}=20$, $\omega_{r1,5,7,11,13}=6.5$, $k_{pi}=50$.

1) Obviously, $G_v(s)$ has large gain in the fundamental and four harmonic frequencies, and zero-error tracking can be achieved in these frequencies [11].

2) With $k_{pv}=0.5, 2.5, 10$, and other parameters unchanged, the frequency characteristics of open-loop voltage transfer function, $G(s)$ and $Z_o(s)$ are shown in figure 3. Figure 3(a) shows that with the increasing of k_{pv} , the bigger the open-loop cut-off frequency will be, the better the system's rapidity will be, but the smaller the phase margin will be, then the system stability is reduced. Figure 3(b) shows that the bigger k_{pv} is, the better voltage tracking will be. Figure 3(c) shows that the bigger k_{pv} is, the smaller magnitude gain of $Z_o(s)$ and gain for each harmonic will be, which will suppress the influence of the harmonic currents for output voltages. Thus, k_{pv} needs to be compromised.



(a) open loop of voltage (b) closed loop of voltage $G(s)$ (c) equivalent output impedance $Z_o(s)$

Figure 3. Bode diagrams with $k_{pv}=0.5, 2.5, 10$

2.2. Droop control

The reference voltage of double closed-loop is generated by droop control and virtual impedance. In low-voltage system with resistance line, droop control equations can be defined into [7,12]:

$$\begin{cases} U_r = U_n - n(P_o - P_n) \\ \omega_r = \omega_n + m(Q_o - Q_n) \end{cases} \quad (4)$$

where P_n and Q_n are the reference active and reactive power with inverter operating in nominal voltage and grid-connected mode; P_o and Q_o are the actual output active and reactive power of inverter; U_n and ω_n are the nominal amplitude and frequency of grid voltage; U_r and ω_r are the reference amplitude and frequency of inverter output voltage. n and m are the droop coefficients of active power-amplitude and reactive power-angular frequency.

In order to reduce the deviations of the inverter output voltage and frequency with traditional droop control in island mode, voltage and frequency error feedbacks are added into droop control equations [1,11], which can be expressed as follows:

$$\begin{cases} U_r - U_n = (k_{pn} + k_{in} / s)(U_n - U_r) - n(P_o - P_n) \\ \omega_r - \omega_n = -(k_{pm} + k_{im} / s)(\omega_r - \omega_n) + m(Q_o - Q_n) + \omega_{sys} \end{cases} \quad (5)$$

where ω_{sys} is pre-synchronize phase signal and will be added to droop control equations in grid-connected mode. In island mode, $\omega_{sys}=0$. P_o and Q_o can be calculated as follows [11]:

$$p = u_{o\alpha} \cdot i_{o\alpha} + u_{o\beta} \cdot i_{o\beta} \quad (6)$$

$$q = u_{o\beta} \cdot i_{o\alpha} - u_{o\alpha} \cdot i_{o\beta} \quad (7)$$

where p and q are instantaneous active and reactive powers. In order to eliminate the ripple of p and q , low-pass filter is used to obtain active power P_o and reactive power Q_o .

Moreover, according to equation (4), the inverter output impedance must be resistive [7]. Thus, virtual impedance is added into double-closed loop to reduce the impact of controller parameters on the inverter output impedance. Virtual impedance can be expressed as follows:

$$Z_v(s) = R_v - sL_v \quad (8)$$

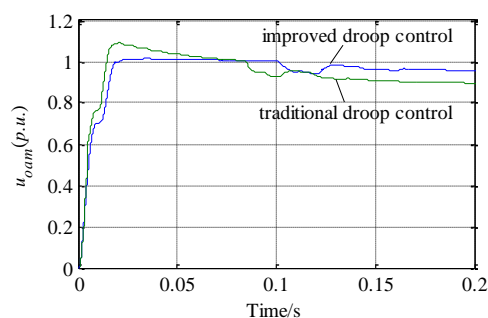
where R_v is the resistance component and L_v is the inductance component. A low-pass filter is added into the virtual impedance to suppress the harmonic interference [11].

3. Simulation Results

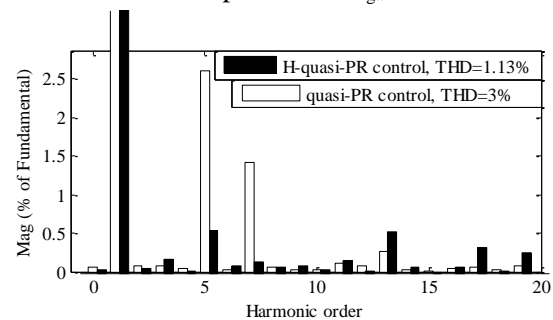
Matlab/Simulink is used to build a three-phase inverter model, as shown in figure 1. The system parameters are: 1) main circuit: $U_{dc}=800V$, $L=5mH$, $r=0.02\Omega$, $C=400\mu F$, $f_s=5kHz$, $U_g=380V/50Hz$; 2) linear load: $P_L=16kW$, $Q_L=0kvar$; 3) rectifier load: $L_{non}=1mH$, $C_{non}=1000\mu F$, $R=20\Omega$; 4) droop control: $n=0.35$, $m=0.02$, $U_r=311V$, $\omega_r=100*\pi$, $P_n=14kW$, $Q_n=0var$, $k_{pn}=300$, $k_{in}=0.05$, $k_{pm}=300$, $k_{im}=0.05$; 5) voltage quasi-PR control: $k_{pv}=1.5$, $k_{r1}=200$, $k_{r5}=150$, $k_{r7}=100$, $k_{r11}=50$, $k_{r13}=20$, $\omega_{r1,5,7,11,13}=6.5rad/s$; 6) current P control: $k_{pi}=50$; 7) virtual impedance: $R_v=0.5\Omega$, $L_v=0.25mH$; 8) pre-synchronization: $k_{pr}=500$, $k_{ir}=50$.

The system starts in island mode with linear load. The rectifier load is added at 0.1s. The operation of pre-connecting to the grid is begun at 0.25s, before connecting to the grid at 0.45s when the grid switch is closed. At 1.5s, the system returns to be island mode when the grid switch is opened.

Figure 4 shows the inverter output voltage and its frequency spectrum analysis waveforms in island mode. Figure 5 shows the inverter output current and voltage frequency waveforms under rectifier load in island mode. Figure 6 shows voltage tracking and the inverter output power in grid-connected mode waveforms. Figure 7 shows the grid current waveforms and FFT spectrum of i_{ga} .



(a) Inverter output voltage magnitude u_{oam} (p.u.)



(b) Frequency spectrum analysis of u_{oa} with rectifier load

Figure 4. Inverter output voltage and its frequency spectrum analysis waveforms in island mode

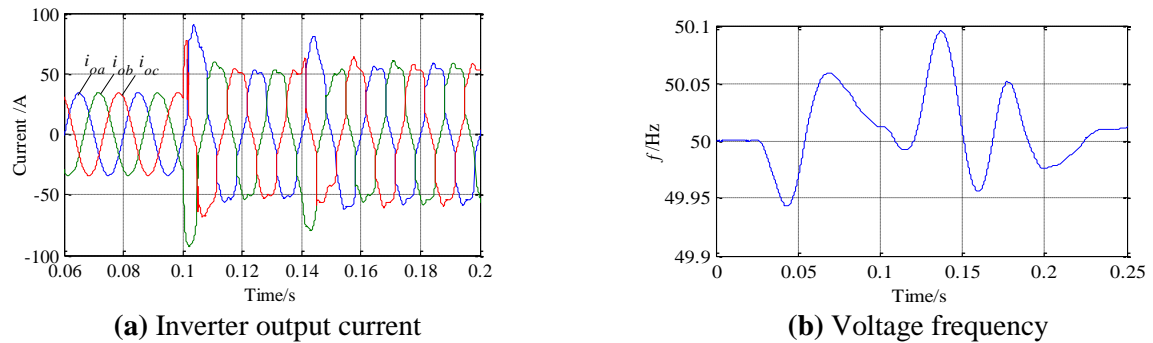


Figure 5. Inverter output current and voltage frequency waveforms with rectifier load added at 0.1s

It can be seen from figure 4(a), that when the rectifier load is added in island mode, the deviation between output and rated voltages with the improved droop control is smaller than that with the traditional droop control. Under rectifier load in island mode, the total harmonic distortion (THD) of output voltage u_{oa} , by harmonic voltage quasi-PR control (H-quasi-PR, THD=1.13% shown in figure 4(b)) is better than the one (THD=3%) without the harmonic resonant control, i.e. $k_{r5}=k_{r7}=k_{r11}=k_{r13}=0$. Figure 5(b) shows that the frequency deviation of inverter output voltage is within ± 0.1 Hz, which is small. In order to limit the current surge at the initial moment when the rectifier load is added, current-limiting resistance is used. Figure 5(a) shows the current surge is relatively small. Therefore, the control scheme proposed in this paper can maintain the inverter output voltage and frequency stability in island mode.

From figure 6(a), after 0.25s, the phase error between inverter output voltage and the grid voltage is eliminated with pre-connecting operation. Figure 7(a) shows that the grid current surge is very small and grid currents enters their stable states within 0.2s. Under rectifier load in grid-connected mode, the grid current THD by harmonic voltage quasi-PR control (H-quasi-PR, THD=3.70% shown in figure 7(b)) is better than the one without the harmonic resonant control (THD=16.7%). The grid current THD=3.7% < 5% meets the grid-connected requirements [13]. Figure 6(b) shows that the inverter stable outputs active power is 14kW and reactive power is 0var in grid-connected mode.

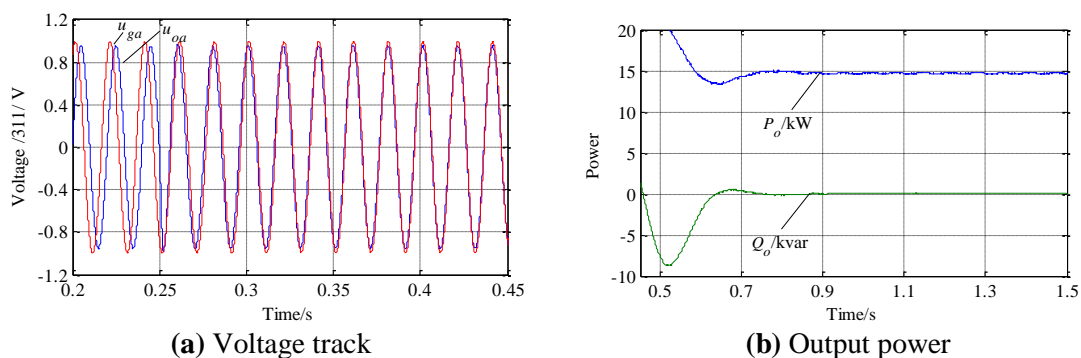


Figure 6. Voltage track at 0.25s and output power in grid-connected mode waveforms

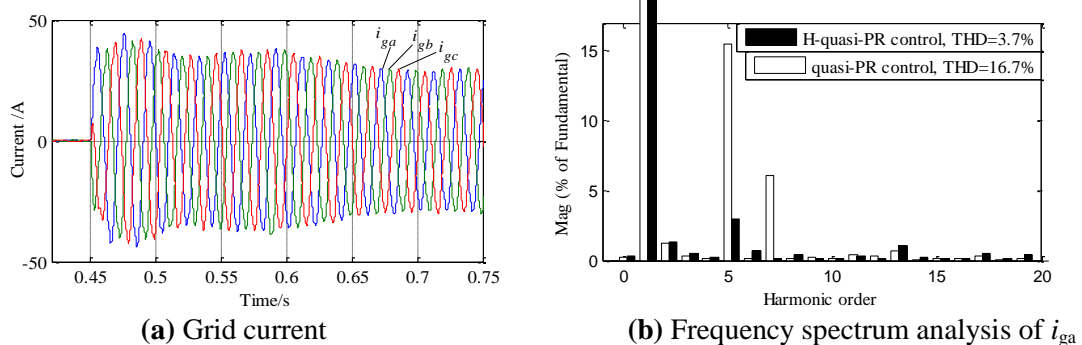


Figure 7. Waveforms of grid current and its frequency spectrum analysis in grid-connected mode with rectifier load

4. Conclusion

This paper proposed an improved droop control scheme with virtual impedance added for three-phase inverter in island and grid-connected modes. Quasi-PR controller based on $\alpha\beta$ stationary coordinate system is used in the voltage and current double closed-loop. Matlab simulation results show that: 1) when microgrid operates in island mode with nonlinear loads, the inverter output voltage distortion is small, and the inverter output voltage and frequency stability can be achieved; 2) when microgrid operates in grid-connected mode, the inverter outputs constant power and the grid current THD meets the grid-connected requirements. Therefore, the control scheme proposed in this paper provides a good performance for the microgrid control system.

Acknowledgments

This work was supported by the Natural Science Foundation of China under Grant 51407084.

References

- [1] J M Guerrero, J C Vasquez, José Matas, et al 2011 Hierarchical Control of Droop-Controlled AC and DC Microgrids—A General Approach Toward Standardization *IEEE Trans. Ind. Electron* vol. **58** pp. 158-172.
- [2] Hisham Mahmood, Dennis Michaelson, Jiang Jin 2015 Decentralized Power Management of a PV/Battery Hybrid Unit in a Droop-Controlled Islanded Microgrid *IEEE Trans. Power. Electron* vol. **30** pp. 7215-7229.
- [3] Hiren Patel and Vivek Agarwal 2008 Control of a Stand-Alone Inverter-Based Distributed Generation Source for Voltage Regulation and Harmonic Compensation *IEEE Trans. Power. Del* vol. **23** pp. 1113-1120.
- [4] S Chen, Y Lai, S C Tan, and C Tse 2008 Analysis and Design of Repetitive Controller for Harmonic Elimination in PWM Voltage Source Inverter Systems *IET Power. Electron* vol. **1** pp. 497-506.
- [5] Q N Trinh, H H Lee 2014 An Enhanced Grid Current Compensator for Grid-Connected Distributed Generation Under Nonlinear Loads and Grid Voltage Distortions. *IEEE Trans. Ind. Electron* vol. **61** pp. 6528-6537.
- [6] R. Ortega, J Sosa, O Carranza and V García 2014 Comparison Controllers for Inverter Operating in Island Mode in Microgrids with Linear and Nonlinear Loads *IEEE Latin America Trans* vol. **12** pp. 1441-1448.
- [7] Yao Wei, Chen Min, José Matas, J M Guerrero 2011 Design and Analysis of the Droop Control Method for Parallel Inverters Considering the Impact of the Complex Impedance on the Power Sharing *IEEE Trans. Ind. Electron* vol. **58** pp. 576-588.
- [8] Alexander Micallef, Maurice Apap and C S Staines 2014 Reactive Power Sharing and Voltage Harmonic Distortion Compensation of Droop Controlled Single Phase Islanded Microgrids *IEEE Trans. Smart Grid* vol. **5** pp. 1149-1158.
- [9] Q C Zhong 2013 Harmonic Droop Controller to Reduce the Voltage Harmonics of Inverters *IEEE Trans. Ind. Electron* vol. **60** pp. 936-945.
- [10] Dipankar De, V Ramanarayanan 2010 Decentralized Parallel Operation of Inverters Sharing Unbalanced and Nonlinear Loads *IEEE Trans. Power. Electron* vol. **25** pp. 3015-3025.
- [11] J C Vasquez, J M Guerrero, Mehdi Savaghebi, et al 2013 Modeling, Analysis, and Design of Stationary-Reference-Frame Droop-Controlled Parallel Three-Phase Voltage Source Inverters *IEEE Trans. Ind. Electron* vol. **60** pp. 1271-1280.
- [12] J M Guerrero, L G Vicuña, José Matas, et al 2005 Output Impedance Design of Parallel-Connected UPS Inverters With Wireless Load-Sharing Control *IEEE Trans. Ind. Electron* vol. **52** pp. 1126-1135.
- [13] IEEE Std 1547-2003, Standard for Interconnecting Distributed Resources with Electric Power Systems.